UCRL 9394

UNIVERSITY OF CALIFORNIA

Ernest O. Lawrence

Radiation Laboratory

N^{15} (p,p2n)N^{13} REACTION INDUCED BY PROTONS OF ENERGY 0.4 TO 6.2 BEV

DISCLAIMER

UCRL-9394
UC-34 Physics and Mathematics
TID-4500 (15th Ed.)

UNIVERSITY OF CALIFORNIA

Lawrence Radiation Laboratory
Berkeley, California

Contract No. W-7405-eng-48

$N^{15}(p,p2n)N^{13}$ REACTION INDUCED BY PROTONS OF ENERGY 0.4 TO 6.2 BEV.

Linda Chang Sah
(Master's Thesis)

August 1960

Printed in USA. Price 75 cents. Available from the
Office of Technical Services
U. S. Department of Commerce
Washington 25, D.C.

$N^{15}(p,p2n)N^{13}$ REACTION INDUCED BY PROTONS OF ENERGY 0.4 TO 6.2 BEV.

Contents

$N^{15}(p,p2n)N^{13}$ REACTION INDUCED BY PROTONS OF ENERGY 0.4 TO 6.2 BEV.

TABLES

$N^{15}(p,p2n)N^{13}$ REACTION INDUCED BY PROTON OF ENERGY 0.4 TO 6.2 BEV.

FIGURES

$N^{15}(p,p2n)N^{13}$ REACTION INDUCED BY PROTONS OF ENERGY 0.4 TO 6.2 BEV.

Linda Chang Sah

Radiation Laboratory and Department of Chemistry
University of California, Berkeley, California

August, 1960

ABSTRACT

N^{14} and N^{15} were bombarded with protons in the energy range 0.4 to 6.2 Bev. Measured values of the absolute cross sections for $N^{14}(p,pn)N^{13}$ is 6 mb over the stated energy range, which agree and supplement the previous measurements[1] up to 3.0 Bev. The (p,pn) yield is higher than the (p,p2n) yield by a factor of 2 to 3 in the entire energy range of interest.

$N^{15}(p,p2n)N^{13}$ REACTION INDUCED BY PROTONS OF ENERGY 0.4 TO 6.2 BEV.

Linda Chang Sah

Radiation Laboratory and Department of Chemistry
University of California, Berkeley, California

August, 1960

INTRODUCTION

It has been observed that the yield of 10-min N^{13} produced in proton reactions in the Bev energy region is low in comparison to other reaction products similarly made.[1] For example, the absolute cross section of $C^{12}(p,pn)C^{11}$ is 30 mb[2] while that of $N^{14}(p,pn)N^{13}$ is only 6 mb. An explanation was given by D. H. Wilkinson[3] who attributed the difference to the assumption that all excited states of N^{13} are unstable with respect to particle emission. That is, all excited states of N^{13} are unstable with respect to proton decay to form C^{12}. Thus, the production of 10 min N^{13} is decreased by the amount that would have been produced if the gamma-ray emission to the ground state was more competative with proton emission. In other words, N^{13} is a particular nuclide which can only be observed as a reaction product by radiochemical techniques when it is formed solely in its ground state. In the case of $N^{14}(p,pn)N^{13}$, this means that in order to observe any N^{13}, the incident proton is able to knock out a neutron from N^{14}, and escape with its collision partner without causing any excitation in the residual N^{13} nucleus.

Experiments are being carried out to compare the probability for producing N^{13} from a direct "knock-on" process, such as $N^{14}(p,pn)N^{13}$, and the probability of producing N^{13} from a "knock-on" followed by evaporation of a single neutron to the ground state, i.e., $N^{15}(p,p2n)N^{13}$. Based on Wilkinson's argument then, the cross section for the $N^{15}(p,p2n)N^{13}$ reaction should be also low in the high energy range. Experimental data are obtained for the cross sections of both the reactions $N^{14}(p,pn)N^{13}$ and $N^{15}(p,p2n)N^{13}$ between 0.4 and 6.2 Bev. The $N^{14}(p,pn)N^{13}$ data are used to check and supplement the previous measurements.[1],[4]

EXPERIMENTAL PROCEDURES

1. Selection and preparation of the target material.

Because of the ease of handling, boron nitride was chosen as the target material. It is rather inert and is neither hydrolyzed nor oxidized to any appreciable extent in air. The objection to the presence of O^{16} lies in the fact that it gives rise to the production of N^{13} and O^{15}; the former being the product sought, the latter, having a 2-min half-life, will make the decay curve resolution more difficult. Furthermore, boron nitride is chosen since the boron-proton reaction would not give N^{13} as product, while a heavier nucleus than nitrogen in place of boron will form additional N^{13} upon high energy proton bombardment. Carbon-containing target materials were also not used because $C^{12}(p,pn)C^{11}$ reaction cross section is large in the Bev region and the 20-min C^{11} will in turn make the decay curve resolution difficult. Objections to Li_3N will be mentioned later.

Since N^{15} was available in gaseous form (enriched to 93.82% in N^{15}), it was allowed to react directly with powdered boron to form boron nitride. The reaction was carried out in an electrically heated 1-mil molybdenum boat at 1600°C in a nitrogen (N_2^{15}) atmosphere. The excess N_2^{15} gas was recovered by trapping on silica gel at -196°C, liquid-nitrogen temperature.

The apparatus is shown in Figure 1. The 2-liter bell jar was evacuated before the reaction in order to outgas the silica gel, molybdenum shield, and boron. The shield was used to protect the bell jar because the heating period was rather lengthy and the reaction temperature was about 1600°C.

An experiment was carried out to determine whether molybdenum can be used for the boat and the heat shield in nitrogen. No appreciable reaction with the boat or absorption by the shield was observed. Tungsten was also tested and was found to react with nitrogen. Therefore, it was not used in the experiment.

After the jar was evacuated and the system outgased (this was indicated by the holding of the vacuum for about an hour or so), nitrogen gas was admitted to react with boron. The silica gel serves as an absorber for temporary storage of the nitrogen. Cooling and warming of the silica gel by inserting or removing the liquid air dewar was also employed with proper opening and closing of the valves to ensure the largest amount of nitrogen gas transport into the bell jar. The molybdenum boat containing the boron powder was subsequently heated to 1600°C to cause the reaction of the boron powder with

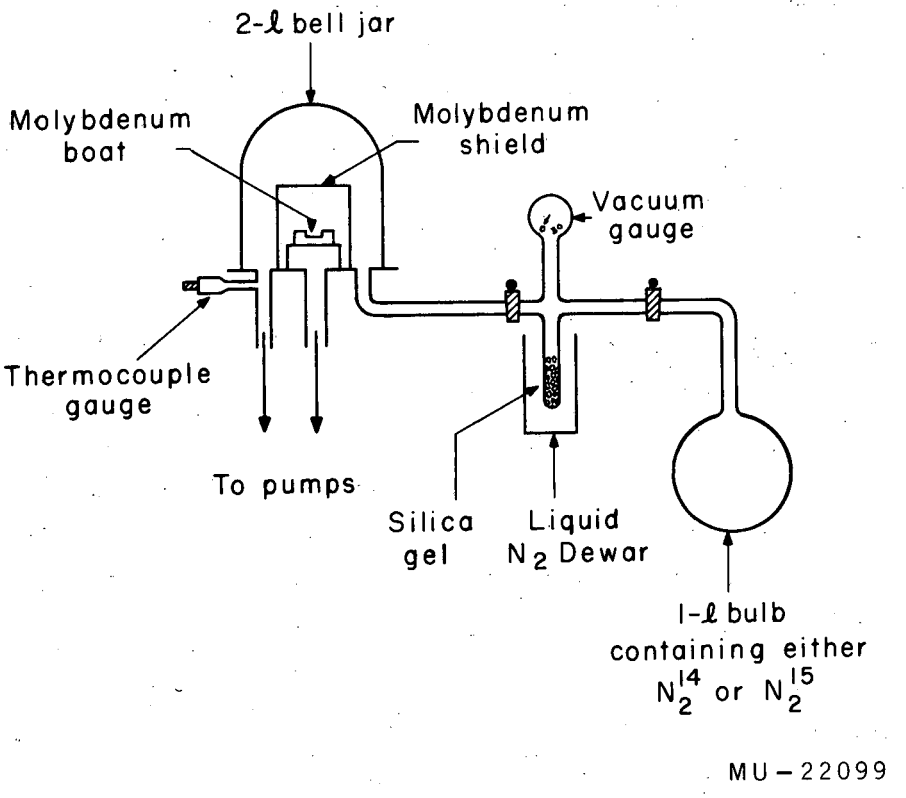

Fig. 1. Apparatus for Boron Nitride Synthesis.

the N_2 gas.

At the end of the reaction, the unreacted nitrogen gas was absorbed into the silica gel by cooling with liquid nitrogen. The pressure in the bell jar fell to about 100μ of Hg pressure after one to two hours; this corresponds to about 0.24 cc of N_2^{15} at STP.

An open-top box was made out of 1-mil molybdenum sheet by gently folding. The arrangement provides a fairly satisfactory good geometry in heat focusing and the reaction was carried out successfully.

The stoichiometric percentage of nitrogen in boron nitride is 56%; the sample made by the above process is usually between 20-40% of nitrogen, the remainder being unreacted boron. The total reaction period per boat of boron (about 200 mg) took about 30 or 40 hours. Change in color from black (the original boron) to white (boron nitride) serves as a rough indication for the progress of the reaction. Since the separation of the product mixture is difficult and the presence of unreacted boron does not interfere with the experiment of interest, the product mixture was used for bombardment. Table 1 shows two typical chemical analyses of the target material.

TABLE 1

CHEMICAL ANALYSIS OF TARGET MATERIAL

Sample	%B	%N	%B ± %N	%O*
$B_3N_3^{14}$	64.2±0.5	35.8±0.1	100±0.5	0.0±0.5
$B_3N_3^{15}$	77.0±0.9	24.0±0.4	101.0±0.9	1.0±0.9

*Assuming the impurities are oxygen.

As the reaction rate of the nitrogen with powdered boron was relatively slow at 1600°C, lithium nitride was prepared as an alternative material. Analysis showed that reaction was complete to form Li_3N. The Li_3N, however, picks up water vapor from the air so rapidly that it was impossible to carry out the bombardment without partial hydrolysis. Furthermore, in an attempt to make it into a pellet form (to both reduce the surface exposure to the atmosphere and to serve as a more convenient target material), several difficulties have been encountered. These arise from the intrinsic properties of metallic lithium

and lithium nitride. Because molten lithium attacks practically all of the common container materials, such as iron, nickel, copper, platinum, silica, and porcelain, etc., molybdenum seems to be the only convenient material which could serve as a container for the direct union of lithium and nitrogen at about 500°C. In addition, lithium nitride forms a hard, porous, puffy lump in the molybdenum boat and a piece of uniform material is hard to obtain. Even when a very small uniform area is obtained, the process of cutting it out from the molybdenum boat is a difficult task due to the difference in hardness between the boat and the nitride. Diamond saw was used, but the cooling agent required to operate the saw necessitates the sample's exposure to air, water vapor, and oxygen. Lithium hydroxide and lithium oxide were formed under all possible precautions. The attempt to use lithium nitride was thus abandoned.

Because a powder does not provide as uniform a target and source for beta counting as a pellet target, several bombardments of $B_3N_3^{14}$ were performed with the target material pressed into pellet forms in order to test the effect of target form on the measured cross sections. Unfortunately, some binding agent, "Zapon", had to be used in the pellet-pressing process, so that both carbon and oxygen were introduced. No binder was used for either the N^{14} or N^{15} powder targets. By analytical means, the added carbon was found to be about 1%, while a reasonable estimation for oxygen is about 0.1% as upper limit. While it is probably a good assumption to neglect the N^{13} produced by $O^{16}(p,2p2n)N^{13}$, the presence of O^{15} from $O^{16}(p,pn)O^{15}$ and the C^{11} from $C^{12}(p,pn)C^{11}$ was rather undesirable from the view point of decay curve resolution. Thus, the pellet target serves merely to check the values of cross sections at different bombarding energies for $N^{14}(p,pn)N^{13}$. The results from powdered and pellet targets were found to agree within 10%.

2. Beam monitor.

In order to measure any absolute cross section, it is necessary to know, or have a measure of, the beam intensity. This can be accomplished by use of charge collection as in low energy bombardments or by use of a reaction whose cross section is known. In this work, the $Al^{27}(p,3pn)Na^{24}$ reaction is convenient because the cross section is fairly well defined in the energy region of interest. The Na^{24} has a 15-hr half-life and emits negatrons of maximum energy 1.39 Mev; its decay properties are sufficiently different from those of other nuclides formed by reaction of protons in the Bev region with Al^{27} so that the disintegration rate may be determined by half-life alone with the use

of a calibrated end-window beta proportional counter. The $Al^{27}(p,3pn)Na^{24}$ reaction cross section is taken to be 10.7±0.6 millibarns from 0.4 to 6.2 Bev[2] throughout the present study.

3. Target assembly.

The irradiation arrangement is shown in Fig. 2. The boron nitride powder is held in place by two 3-mil aluminum foils in an indented envelope (1 cm x 0.5 cm). Two additional 3-mil aluminum foils are placed behind the envelope. The foil which is used to monitor the proton beam is that part of foil 3 (see Fig. 2) which lies directly behind the area covered by the powder. Foil 3 is thus "sandwiched" between two 3-mil foils and recoil loss of Na^{24} from foil 3 is compensated by the same recoil gain from Nos. 2 and 4.

All the irradiations between 0.4 Bev and 0.72 Bev were performed at the Berkeley 184-inch synchrocyclotron while those between 2.0 Bev and 6.2 Bev were carried out at the Berkeley Bevatron. The target assemblies for the two accelerators are shown in Figs. 3 and 4. The foils are carefully aligned to minimize errors caused by non-uniform beam distribution over the target area.

4. Recoil Considerations.

a. Loss of N^{13} from the boron nitride:

The thickness of the powder was 20 to 30 mg/cm^2. Previous studies[3] have shown that the recoil loss of F^{18} produced by the similar $F^{19}(p,pn)F^{18}$ reaction (in the Bev energy region) from "Teflon", $(CF_2)_n$, foils of thickness 2.7 mg/cm^2 is about 3±1%. Because the targets used in the present experiment were about ten times thicker than the Teflon, the fraction of N^{13} which recoiled out of the boron nitride was considered to be negligible.

b. Possible addition of N^{13} from the $Al^{27}(p,7p8n)N^{13}$ reaction:

Because the boron nitride powder was "sandwiched" between two 3-mil aluminum foils, it was possible for some N^{13} produced by proton reactions in these foils to recoil into the powder; this would increase the observed yield of N^{13}. The magnitude of this increase is taken to be 3±1% for the following reasons:

(1) Direct counting of boron nitride powder itself indicated that the activity of 15-hr Na^{24} was about 0.004 of the activity of the 10-min N^{13}, at end of bombardment. It is known[3] that the ratio of N^{13} atoms compared to Na^{24} atoms produced in aluminum by protons in the Bev region is about 0.1. If it is assumed that the recoil ranges of N^{13} and Na^{24} in aluminum are the same, then the ratio of recoil activities is 0.1 x 900-min/10-min or 9. Therefore,

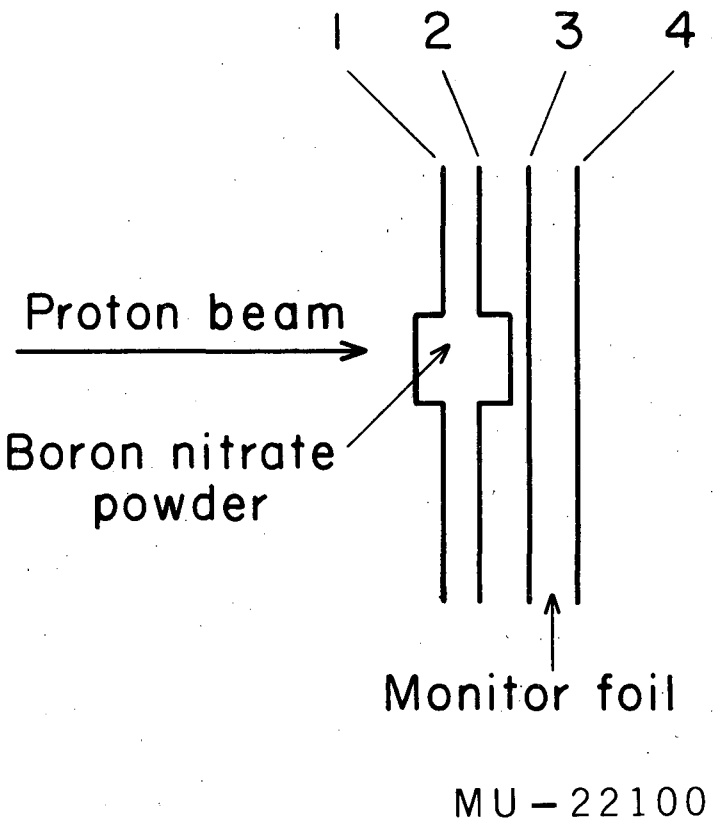

Fig. 2. Target foil arrangement.

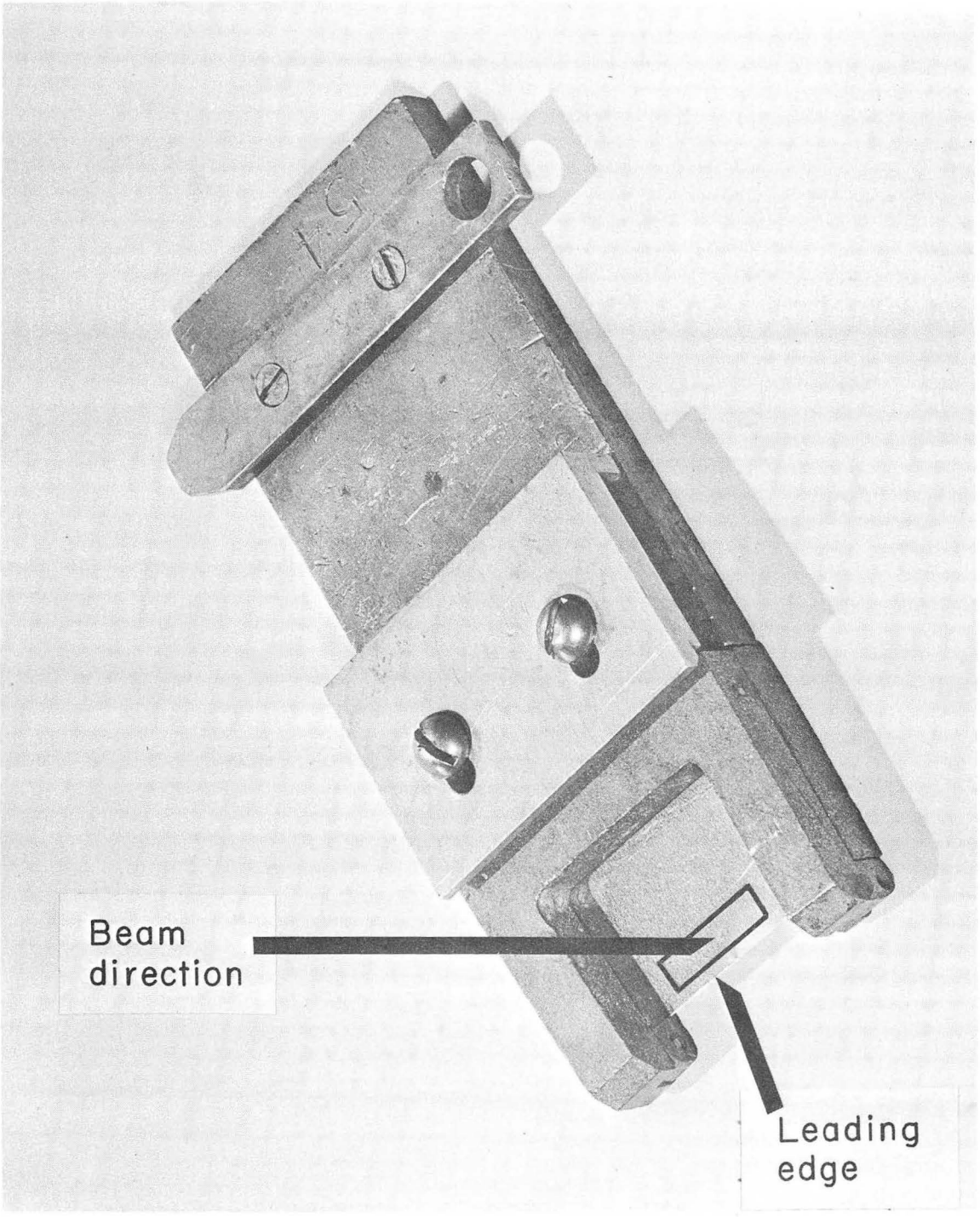

ZN-2618

Fig. 3. 184-inch synchrocyclotron target holder.

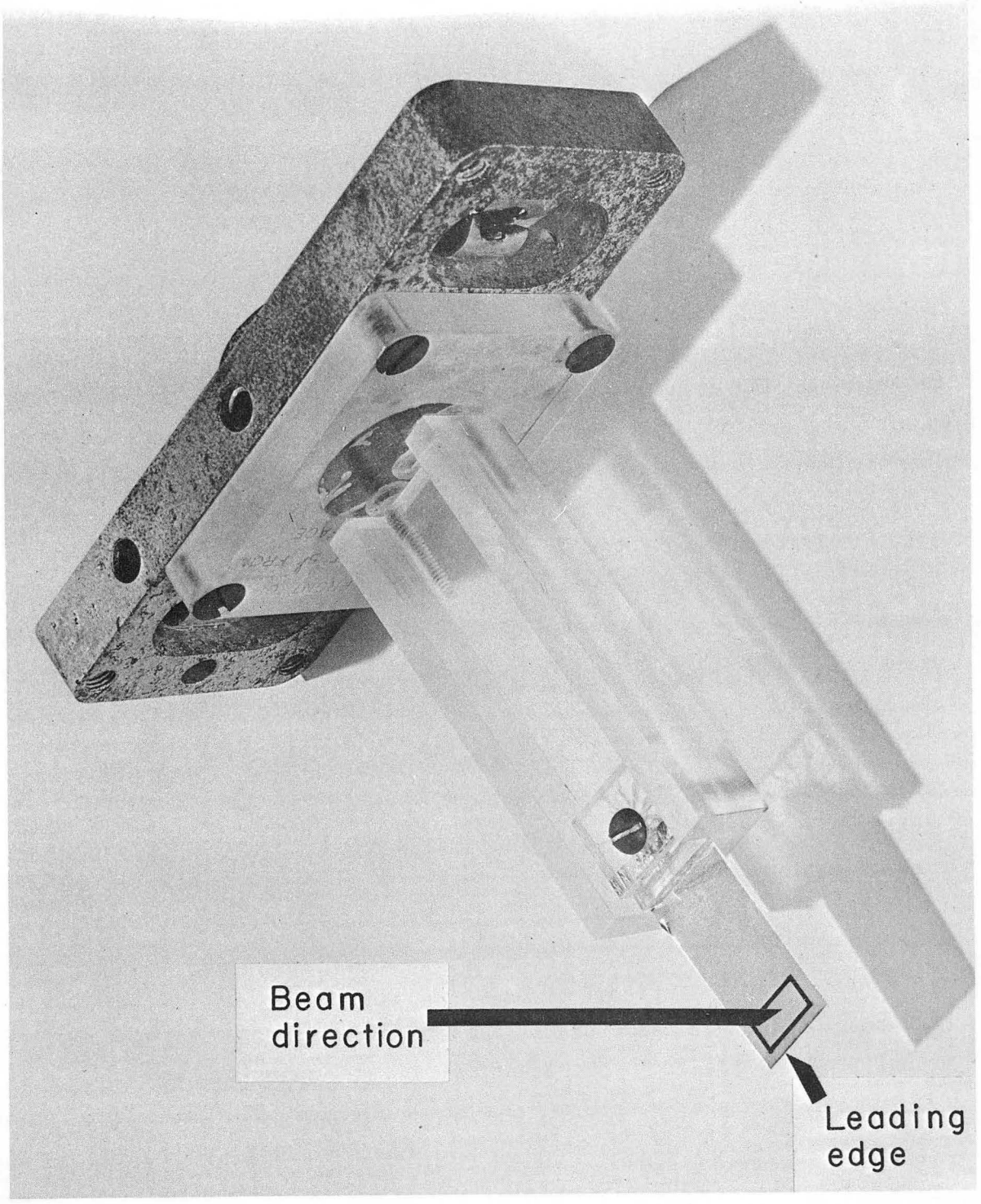

ZN-2619

Fig. 4. Bevatron target holder.

the ratio of activity of N^{13} recoiling into the boron nitride is 0.004 x 9 or 0.036 of the total N^{13} activity detected.

(2) By a similar procedure involving the activity of 112-min F^{18} production in aluminum[3] in the Bev energy region, the amount of N^{13} recoil gain was calculated to be about 4%.

(3) Sugerman[3] has shown that the recoil loss of Be^{7} produced by interaction of Bev protons with 0.003-inch aluminum is a few percent.

This 3% recoil gain correction is included in the N^{13} results shown in Table 2. The correction, although small, could have been avoided by interposing a polyethylene "catcher" foil between the aluminum and the powder. This, however, would have increased the decay-curve resolution because of the comparatively large amount of 20-min C^{11} which would recoil out of the polyethylene into the boron nitride, the C^{11} production cross section being about 30 mb[2] from $C^{12}(p,pn)C^{11}$ as compared to 1.8 to 5.3 mb from Al^{27} in the Bev energy range.[3] The use of beryllium as a cather was somewhat inconvenient because of its brittleness.

5. Radioactivity measurements.

After each bombardment, the target was delivered as quickly as possible and the target foils cut apart. The leading edge (about 1 mm), which contained no boron nitride, was rejected. The powder was transfered to an aluminum counting card, 320 mg/cm^2 thick, which is a saturation backscatterer for the positrons from 10-min N^{13}. The powder was spread as uniformly as possible over a 1 x 0.5 cm area in a depression in the card. (This gave the same area and surface thickness (about 20 mg/cm^2) as the portion of the aluminum target foil no. 3 which was used for Na^{24} detection in monitoring the beam). The transfer of the powder to the counting card was quantitative.

The samples were covered with 0.95 mg/cm^2 of "Videne", a rubber hydrochloride plastic, and counted on the fourth shelf (1.5 cm from the window) of an end-window, methane gas-flow, beta proportional counter. About eight to ten minutes elapsed from end of bombardment to the first count.

The decay of the samples was followed for about 50 hours. Activities detected were 2.1-min O^{15}, 10-min N^{13}, 20.5-min C^{11}, 112-min F^{18} and 15-hr Na^{24}. The N^{13} and C^{11} were mainly produced from reactions with N^{14}, or N^{15} in the enriched targets. The F^{18} and Na^{24} were produced in the aluminum envelope and recoiled into the boron nitride. The O^{15} was produced mainly from the oxygen impurity in the nitride and partly from recoils from the aluminum. Analysis of the decay curves indicated that, on the average, the activity of 2.1-min O^{15} was

about six times the activity of 10-min N^{13} at end of bombardment. This "proton activation analysis" shows that the maximum O^{16} impurity that would be present in the boron nitride is about 1.3%, the $O^{16}(p,pn)O^{15}$ cross section being 33 mb.(5)

In a separate experiment at 720 Mev, a stack of three polyethylene, and three "Mylar" foils, and an aluminum monitor foil were irradiated in order to measure the N^{13} produced from O^{16}. It was thus known how much O^{16} impurity could be tolerated in the boron nitride without introducing appreciable error. The Mylar, a polyester plastic, was analyzed and found to contain 4.00% H, 62.58% C, and 33.4% O (by difference). The $O^{16}(p,2p2n)N^{13}$ cross section (corrected for the N^{13} produced from $C^{13}(p,n)$ reaction as determined from the $(CH_2)_n$ foils) was measured to be 0.9 mb. Therefore, it was safe to neglect the N^{13} produced by the (maximum of) 1.3% oxygen impurity in the boron nitride.

6. Determination of the overall detection coefficients.

a. Na^{24}

The overall detection coefficient, which is defined simply as the number by which the count rate is divided to obtain the disintegration rate of a source, for the decay of Na^{24} produced in three-mil aluminum was previously determined to be 0.149(6) on shelf four of the counters. This number was checked by β-γ coincidence count of the Na^{24} sample mounted in an identical manner to those used in the normal irradiations. The results checked within a few percent.

b. N^{13}

The overall detection coefficient for N^{13}, which emits positrons in 100% of its decays, was measured by comparison of the annihilation radiation emitted by a N^{13} source with that emitted by a Na^{22} source whose positron emission rate was known. The Na^{22} standard was supplied by Nuclear Science and Engineering and its strength was checked to within 0.5% by 4x beta counting a thin, "weightless" source.

The N^{13} for this counter calibration was prepared free of all other radioactivities by bombardment of a stack of polyethylene foils with 10 Mev protons at the 60-inch cyclotron. The reaction was $C^{13}(p,n)N^{13}$. It is taken as a reasonable approximation that the efficiency of the counter for positrons emitted from N^{13} imbedded in $(CH_2)_n$ is the same as that for positrons emitted from N^{13} in B_3N_3 at similar surface thicknesses; $(CH_2)_n$ has average Z = 5.3 and B_3N_3 has average Z = 5.7.

The overall detection coefficient for a given beta radiation will vary with the sample thickness because of self-scattering and self-absorption effects. By use of the N^{13} in the polyethylene foils, the variation was found to be small

at the thicknesses used (20-30 mg/cm^2) in the boron nitride high energy bombardments. Table 2 shows the results of self-scattering and self-absorption on shelf 8 of the end-window proportional counter. Overall detection coefficients for other shelves were determined by comparison of the sample counting rate on that shelf with the rate on shelf 8.

TABLE 2

VARIATION OF OVERALL DETECTION COEFFICIENT WITH SAMPLE THICKNESS

Polyelthylene thickness (mg/cm^2)	Overall detection coefficient (shelf 8)
5.0	0.0185 ± 2%
10.0	0.0202 ± 2%
15.0	0.0200 ± 2%
20.0	0.0196 ± 2%
25.0	0.0196 ± 2%
30.0	0.0191 ± 2%

Because the variation is small with sample thicknesses in the 20-30 mg/cm^2 range, errors introduced by the technique used for beta counting the boron nitride powder, which produces a relatively non-uniform surface thickness, are neglected.

RESULTS

1. Calculations of the N^{13} cross sections.

The number of counts per minute at end of bombardment, A^o, was obtained from the decay curve by resolution of the 10-min N^{13} from the other activities (mainly 20.5-min C^{11}) detected. This was done by making decay curve analysis first by hand and then with the aid of an IBM-704 least squares program called "Frenic" which was prepared by R. H. Moore at Los Alamos and modified by R. W. Hoff and J. O. Rasmussen. The least squares program gave the A^o of each component and its standard deviation.

The number of disintegrations per minute at end of bombardment, D^o, was obtained from A^o by the simple relationship

$$D^o = \frac{A^o}{ODC}$$

where ODC is the overall detection coefficient defined by the above equation. The ODC thus includes effects of geometry, window absorption, air absorption, backscattering, self-scattering, self-absorption, inherent counter response to the radiations, and decay scheme. D_{sat} from D^o, the saturation activity in disintegrations per minute, was obtained from:

$$D_{sat} = \frac{D^o}{1 - e^{-0.693\Delta t/t_{1/2}}}$$

where Δt is the length of bombardment in minutes, $t_{1/2}$ = 10.0 min. Bombardments were usually short (about 1 minute) compared to the half-life, so small effects of the variation of the beam intensity during the run were neglected. The cross section is given by:

$$\sigma_{N^{13}} = \frac{D_{sat}(N^{13})}{D_{sat}(Na^{24})} \times \frac{n\,(Al^{27})}{n\,(N^{15} \text{ or } N^{14})} \times \sigma_{Na^{24}}$$

$\sigma_{Na^{24}}$ is the cross section for $Al^{27}(p,3pn)Na^{24}$ taken to be 10.7 mb in the energy range in this study.

n is the number of target atoms per cm^2.

2. Summary of results.

The cross sections are presented in Table 3 and 4, and the excitation functions are shown in Fig. 5.

TABLE 3

CROSS SECTION FOR $N^{14}(p,pn)N^{13}$ REACTION

Energy of Incident Protons (Bev)	Cross Section (mb)
0.4	5.2, 5.3
0.6	4.1, 5.4
0.72	3.8[a], 4.1, 4.6
2.0	5.1[a]
4.1	5.6, 5.7
6.2	4.8, 4.8

TABLE 4

CROSS SECTION FOR $N^{15}(p,p2n)N^{13}$ REACTION

Energy of Incident Protons (Bev)	Cross Section (mb)
0.4	1.8, 2.4
0.6	1.9, 2.4[a], 2.7
0.7	1.6
0.72	2.3, 3.1[a]
2.0	1.7, 2.0
4.1	3.3, 3.5, 3.7
6.2	2.2, 2.2[a]

[a] Pressed pellet target.

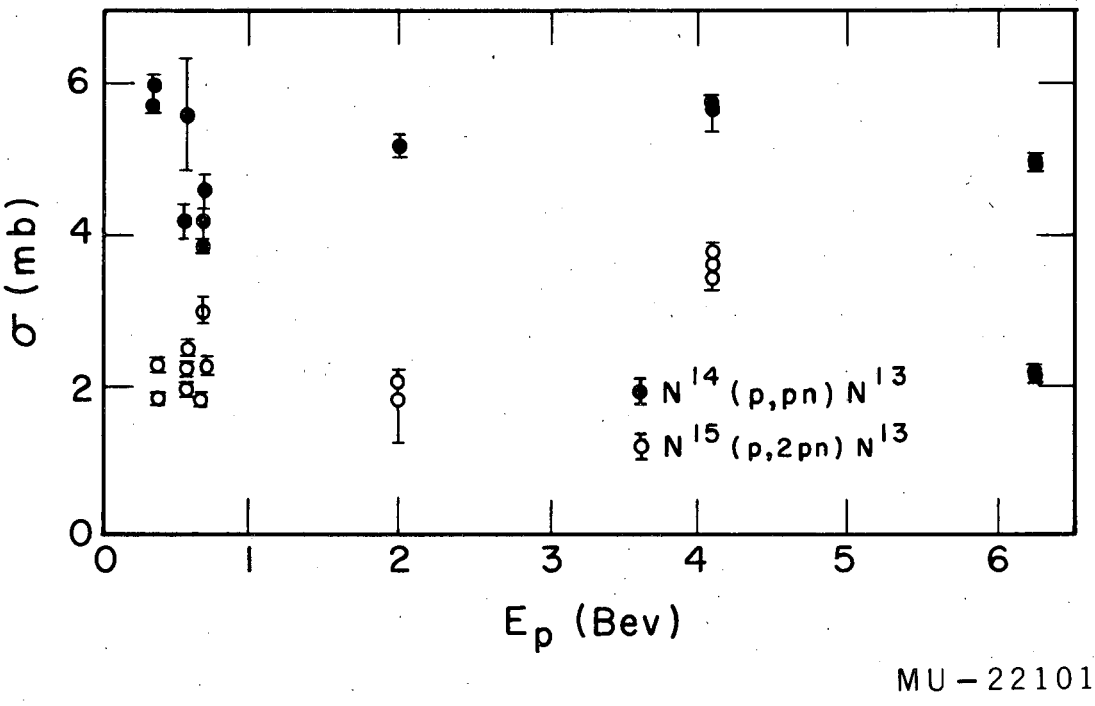

Fig. 5. Excitation function for N^{14} (p,pn)N^{13} and N^{15}(p,p2n)N^{13} in the Bev region. Error flags represent the Standard Deviation given by the IBM-704 decay curve resolution.

All the tabulated N^{13} cross sections were corrected for the following:

a. The 3% contribution of N^{13} which was produced in the aluminum monitor foil and which recoiled into the boron nitride.

b. The production of N^{13} from N^{14} present in the enriched N^{15} boron nitride target. The N_2^{15} gas was analyzed mass spectrometically and found to be 93.82% N^{15} and 6.18% N^{14}. The $N^{14}(p,pn)N^{13}$ cross sections in Table 3 were used to subtract this N^{13} contribution, which amounted to a 6% correction on the average.

3. Errors.

a. Systematic:

(1) From $Al^{27}(p,3pn)Na^{24}$ cross section: a shift of value in this cross section determination will cause the corresponding shift of our σ vs. E curves. The accuracy of this cross section is 6%, i.e., 10.7 ± 0.6 mb.[2]

(2) Overall detection coefficient: It is estimated to be 0.0196 on shelf 8 of the end-window proportional counters. This value was determined to be within 2% by the writer.

b. Random:

(1) Decay curve analysis: The standard deviation computed by the IBM-704 program varied from 1 to 8% for a given N^{13} activity at end of bombardment. The Na^{24} monitor activity is accurate to about 2%.

(2) Uniformity of target and source thicknesses: The non-uniformity of surface thickness of the boron nitride powder target is a source of random error. Another source is the lack of reproducibility of the thickness of the sample used for beta counting.

(3) Energy spread of the proton beams: The energy spread of the beam in the 184-inch synchrocyclotron ranges from the maximum energy down to within 10% of that energy. The Bevatron energy spread is about 1%. The observed cross sections are relatively insensitive to energy in the Bev region.

A measure of the precision of the experiments can be obtained by inspection of the individual results listed in Table 3 and 4.

DISCUSSION

As indicated in Fig. 5, both the $N^{14}(p,pn)N^{13}$ and $N^{15}(p,p2n)N^{13}$ reaction cross sections are fairly energy independent from 0.4 to 6.2 Bev. The $N^{15}(p,p2n)N^{13}$ cross section appears to have a maximum at 4.1 Bev, where that of the $N^{14}(p,pn)N^{13}$ has a smaller maximum.

a. Possible (p,p2n) mechanisms: High energy reactions are generally thought to proceed by two steps; one an initial fast cascade, followed by an evaporation of nucleons. The following mechanisms for the (p,p2n) and (p,pn) reactions will be discussed with this in mind.

(1) Possibility of pure knock-on for (p,p2n) reactions: The probability of a cascade in which a proton strikes a neutron which in turn strikes another neutron and which then leaves the N^{13} residue without excitation is thought to be very unlikely. From Monte Carlo calculation,[7] (on heavier nuclei) it is known that as more particles are ejected in the initial cascade, the average excitation in the cascade residue increases. Such a cascade, therefore, would cause the evaporation of further nucleons and the (p,p2n) product would not be observed.

(2) The mechanism that is more likely is one in which the incident proton strikes a neutron and both cascade out leaving the cascade residue excited to about 8 to 18 Mev. The second neutron is then evaporated leaving the product nucleus with excitations below the threshold for emitting another nucleon. Excitation energy is then carried off by gamma radiation which maintains the integrity of the final product.

(3) From the radiochemical observation, the contribution of the (p,dn) reaction to the observed (p,p2n) reaction cannot be determined. Deutarons have been observed[8] in high energy interactions and have angular distribution consistant with an indirect pickup process in which an incident proton, for example, strikes a neutron. The scattered proton, at lower energy, then may pick up a neutron to form the deuteron. It is assumed for this paper that such process would cause sufficient excitation to destroy the (p,dn) residue nucleus and the (p,dn) contribution therefore, is assumed to be negligible.

(4) Mesons: At energies above the pion threshold, reactions such as $(p,p2n\pi^{o})$ and $(p,2pn\pi^{-})$ become possible. All the collision partners will escape, either in the initial collision or by evaporation followed by deposition of excitation energy.

b. Treatment of $N^{15}(p,p2n)N^{13}$ reaction: Because of the small number of nucleons in N^{15}, it is felt that evaporation and Monte Carlo calculations will not be applicable. The previous Monte Carlo calculation[7] for the cascade particle, such as $N^{15} + p \rightarrow N^{14*} + p + n$, have dealt with heavier target nuclei than N^{15}. What is presented here is a calculation of the expected $N^{15}(p,p2n)N^{13}$ cross section based upon certain analogies with other high energy processes.

The fact that the (p,p2n) reaction cross section of interest should have an energy independent character in the Bev region can be visualized if the reaction as a whole is broken into two steps. The first step consists of a direct knock-on (p,pn) reaction which is relatively independent of energy in the high energy range. This constancy of cross section in the Bev range has been observed for many other (p,pn) reactions involving heavier nuclei, such as: $I^{127}(p,pn)I^{126}$ (9), $Zn^{64}(p,pn)Zn^{63}$ (1), $Cu^{63}(p,pn)Cu^{62}$ (1), $Ni^{58}(p,pn)Ni^{57}$ (1) and $Fe^{54}(p,pn)Fe^{53}$ (1). In the second step, a neutron is evaporated in the de-excitation of the excited nuclei. The probability of the second step is proportional to the integrated cross section over the entire excitation energy range and is a constant. Thus, the final reaction cross section for the (p,p2n) process, which is proportional to the product of the cross sections of the two processes, is independent of proton bombarding energy in the Bev region.

To provide an explanation for the experimentally measured cross section of the $N^{15}(p,p2n)N^{13}$ reaction, the reaction and the decay scheme shown in Fig. 6 may be used to facilitate the discussion. In order to simplify the discussion then, all reactions other than (p,pn) and (p, p2n) are neglected. The interaction of high energy proton with N^{15} may proceed along two routes. (a) The incident proton may make a head-on collision with the nucleons in the N^{15} nucleus by a knock-on (p,pn) reaction following the route (1) shown in Fig. 6 and leave the product N^{14*}. (b) The incident proton may skim the surface of the N^{15} nucleus and interact with a neutron by a knock-on (p,pn) reaction. Since very little energy is transfered to the interior of the nucleus in this process, the resulting nucleus N^{14} is left in the ground state. This process is indicated as (2A) in Fig. 6. Process (2A) or (2B) which resulted from de-excitation of N^{14*} by gamma ray emission cannot be investigated readily by experiments since N^{14} is stable. An estimate of the cross section, however, is possible from other (p,pn) reactions in the light mass region. It has been measured[5] that the (p,pn) reaction cross section is about 30 ± 5 mb over a wide range of the light nuclides, regardless of the oddness and eveness of each nuclide, with the exception of $N^{14}(p,pn)N^{13}$. For example: $C^{12}(p,pn)C^{11}$ (10),(2),

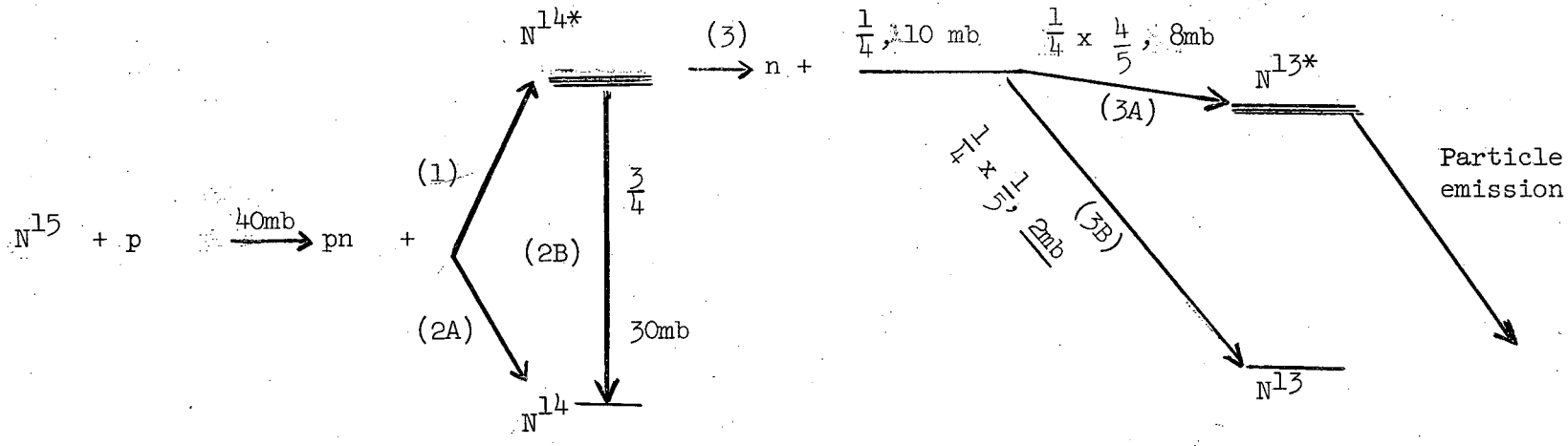

Fig. 6. Interaction Scheme of Bev p with N^{15}, The underlined cross sections are experimental results, others are estimated values.

$O^{16}(p,pn)O^{15}$ (5), $F^{19}(p,pn)F^{18}$ (1),(5),(11),(12), and $Na^{23}(p,pn)Na^{22}$ (1). Thus, the reaction cross section for $N^{15}(p,pn)N^{14}$ is assumed to be approximately 30 mb. Since the process (2A) as shown in Fig. 6 is rather improbable compared with the process (2B) in the high energy range, it is reasonable to assume that the reaction $N^{15}(p,pn)N^{14}$ follows the route (1) and (2B). Thus, $\sigma(2B) = 30$ mb.

The $N^{15}(p,p2n)N^{13}$ reaction results from the N^{14*} nuclei, which had high enough excitation energy and which would decay by neutron evaporation may be estimated from several other (p,pn) and (p,p2n) reactions which have already been investigated; for example: I^{127}, Zn^{64}, Cu^{63}, Ni^{58}, and Fe^{54}. The reaction I^{127} + p will be taken as an example, although a similar argument may be applied to the other medium weight nuclei cited. The reason for the preference of Iodine reaction is that it is the only one that has been carried out throughout the same energy range as the present work and that each cross sectional value has been checked by different methods. The interaction scheme of I^{127} with high energy protons is shown in Fig. 7. The underlined cross sections indicated on the graph are published experimental values.(9) For the $I^{127}(p,pn)I^{126}$ reaction, the total cross section is about 60 mb in the Bev region. Since process (2A) is rather improbable compared with (2B) as discussed previously for N^{15}, it may be assumed that $\sigma(2B) =$ 60 mb. The reaction cross section for $I^{127}(p,p2n)I^{125}$ has also been measured and was found to be around 20 mb in the Bev region.(9) This reaction is assumed to involve first a knock-on (p,pn) reaction followed by neutron evaporation as indicated by route (3) shown in Fig. 7. Thus, the fraction of I^{126*} which has high enough energy to decay by neutron evaporation is about 20 mb/(20 + 60)mb = 1/4. For other nuclei, this ratio varies between 0.16 and 0.33 as obtained from Fig. 8. Thus, we may assume that the fraction of N^{14*} which has high enough energy to proceed by neutron evaporation is also about 1/4. Thus, the cross section for the process following route (3) for nitrogen is about 1/4 x (30 mb/(3/4)) = 10 mb as shown in Fig. 6. The total reaction cross section for (N^{15} + p), considering only (p,pn) and (p,p2n) processes, is 10 mb + 30 mb = 40 mb.

The major differences between $N^{15}(p,p2n)N^{13}$ reaction and other (p,p2n) reactions cited, in addition to the mass differences or differences in number of nucleons, lie in the peculiarity of the energy levels of the end product N^{13}. As has been proposed(3), the first excited level of N^{13} separates from the ground state with a rather large energy gap so that N^{13*} decays most likely by particle emission. Thus, the interaction and decay scheme along route (3) shown in Fig 6 is constructed for nitrogen reactions. In the usual case such as I^{127} shown in Fig. 7, the excited end product, I^{125*}, decays to ground state I^{125} by gamma ray

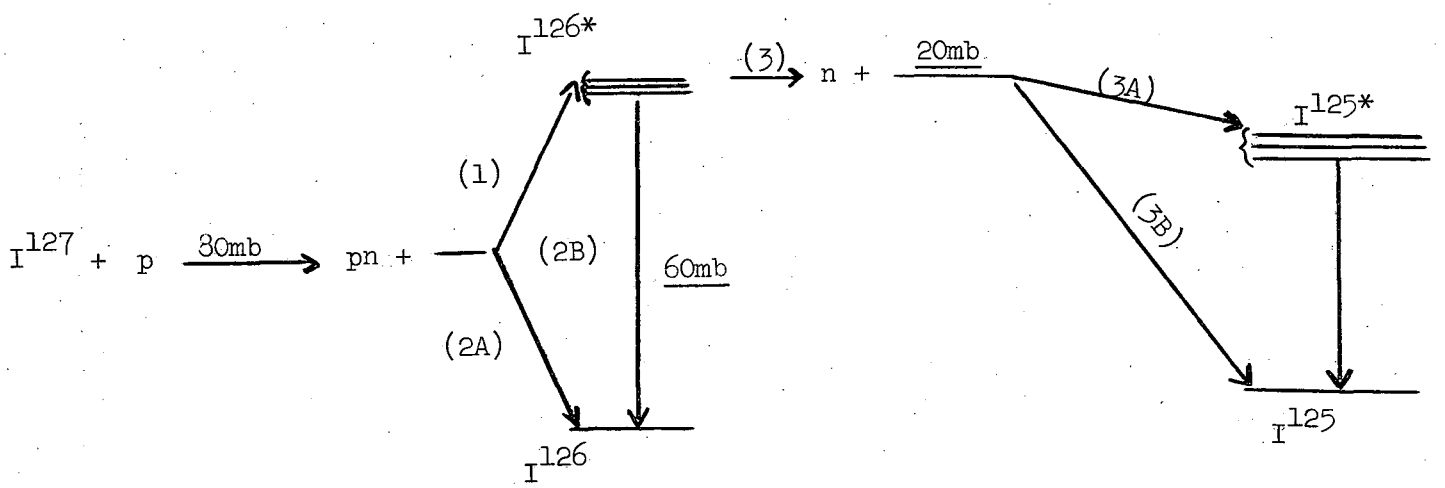

Fig. 7. Interaction Scheme of Bev p with I^{127}. The underlined cross sections are experimental results; others are estimated values.

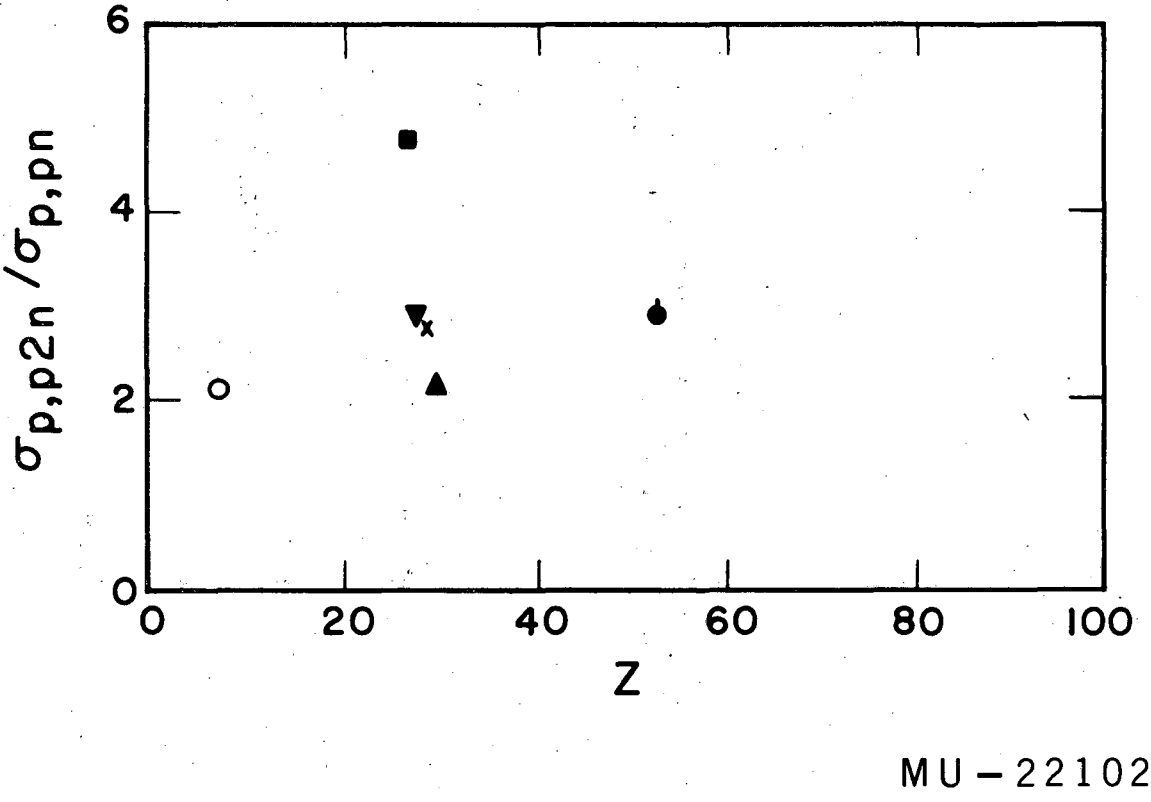

Fig. 8. $\frac{\sigma(p,pn)}{\sigma(p,p2n)}$ vs. Z plot for several nuclei.

emission because of the small energy separation between the ground state and the first excited state.

From these considerations, it is evident that in the $N^{15}(p,p2n)N^{13}$ reaction, it is necessary to know the fraction of the highly excited N^{14*} which decay by neutron evaporation directly to the ground state of the end product N^{13} since the transition $N^{13*} \xrightarrow{\gamma\text{-ray}} N^{13}$ is rather improbable due to the competition of particle emission. In order to make an estimate of this fraction, we may compare the two processes $N^{14}(p,pn)N^{13}$ and $N^{15}(p,pn)N^{14}$. The interaction scheme of these two reactions are shown in Fig. 9. The cross section of the reaction $N^{14}(p,pn)N^{13}$ is obtained from the present and prior experiment and is found to be about 6 mb. As indicated in Fig. 9, N^{13*} decays by particle emission so that the total cross section of the $N^{14}(p,pn)N^{13}$, taking into account both decay to the excited and ground states of N^{13}, must be greater than 6 mb. An estimate of the total cross section may be obtained from the second reaction shown in Fig. 9, $N^{15}(p,pn)N^{14}$, in which the total cross section of 30 mb was estimated previously. Published experimental values for similar reaction pairs such as $Cu^{63}(p,pn)Cu^{62}$ and $Cu^{65}(p,pn)Cu^{64}$ showed almost the same value for the reaction yield of cross section over a wide high energy range. Thus, we may assume that a similar situation holds for the two nitrogen-proton reactions. Thus, the total cross section for formation of the ground and excited state of N^{13} from the reaction $N^{14}(p,pn)N^{13}$ is estimated to be about 30 mb, which was indicated in Fig. 9. Of the total of 40 mb, approximately 6 mb or 1/5 of the end product N^{13} is in the ground state while 24 mb or 4/5 of the end product is in the excited state N^{13*} and decays by particle emission. We may assume that in the $N^{15}(p,pn)N^{14}$ reaction, this ratio is approximately correct. Thus, 1/5 of N^{14*} decays to the ground state N^{13} by neutron evaporation (route (3B) in Fig. 6) while 4/5 of N^{14*} has high enough excitation energy so that after the neutron is evaporated, the end product is left in the excited state, N^{13*}, which subsequently decay by particle emission. Thus, the reaction cross section for $N^{15}(p,p2n)N^{13}$ is expected to be 40 mb x 1/4 x 1/5 = 2 mb which is in excellent agreement with our experimental measurements.

c. An independent experiment was carried out to study the mechanism by which N^{14*} decays to N^{13} ground state. The experiment was designed to compare the N^{14*} compound nucleus formed by a low energy reaction at around 10 Mev with the N^{14*} which is supposedly to be the residual excited nucleus after the first step of the $N^{15}(p,p2n)N^{13}$ reaction, in which N^{14*} is formed from $N^{15}(p,pn)N^{14*}$. The experiment involved the reaction $C^{13}(p,n)N^{13}$ (10-min N^{13} ground state) in which the

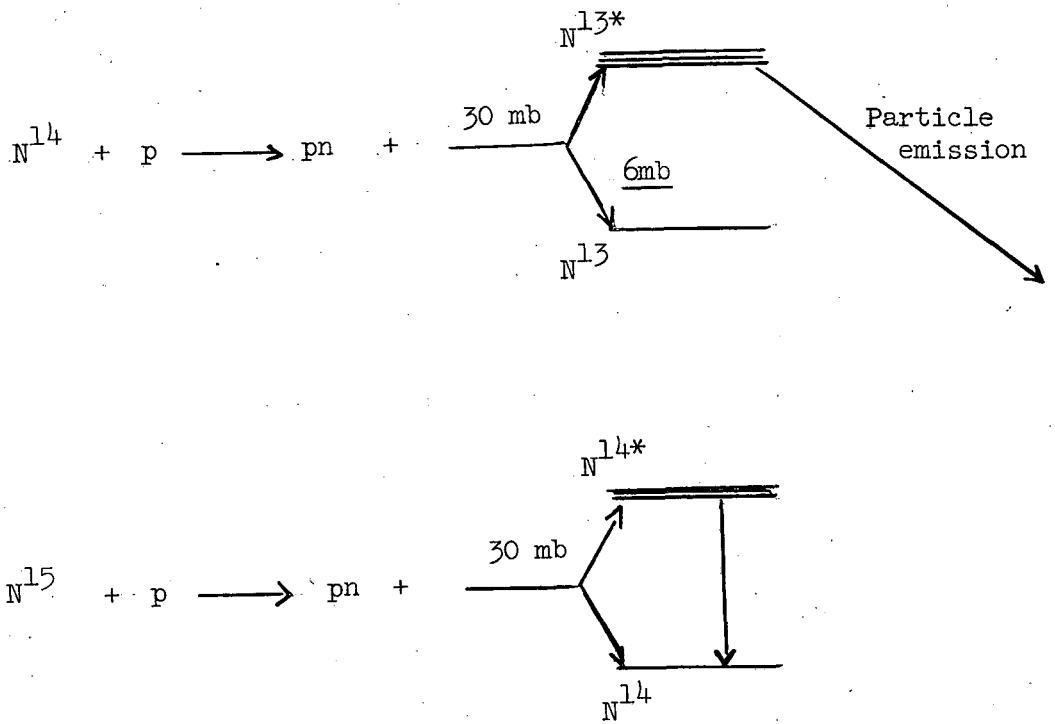

Fig. 9. (p,pn) Reaction of N^{14} and N^{15} at high energies. The underlined cross sections are experimental results; others are estimated values.

N^{14*} compound nucleus was assumed to form in the first step from $C^{13} + p \rightarrow N^{14*}$. In the actual experiment, polyethylene foils were bombarded with protons of energies from 0 to 12 Mev at the 60-inch cyclotron. The proton energy degradation was obtained by placing 3-mil aluminum foils sandwiched in between the polythylene foils. The energy is such that the reaction was $C^{13}(p,n)N^{13}$ or $C^{13} + p \rightarrow N^{14*} \rightarrow N^{13} + n$, which was evidenced in the decay curve resolution in which only the 10-min N^{13} was observed.

The cross section vs. proton energy is plotted in Fig. 10. An "average" cross section for the reaction $C^{13}(p,n)N^{13}$ (ground state N^{13} only) was obtained from:

$$\sigma = [1/(E_{max} - E_{min})] \cdot \int_{E_{min}}^{E_{max}} \sigma(E_p) dE_p$$

by graphical integration of Fig. 10, where E_{max} and E_{min} corresponds to the two energy cut-off points. This calculation yields 100 mb for the decay of the compound nucleus N^{14*} to the ground state N^{13} by neutron emission. The geometric cross section of N^{14} is 409 mb, so that the probability of the transition is 100 mb/409 mb or about 1/4. The product of this fraction and the cross section for $N^{15}(p,pn)N^{14*}$ (which is estimated to be 30 mb previously) would give 1/4 x 30 mb or about 7 mb which is obviously too high compared with the experimental values of 2 mb. Therefore, it is concluded that the N^{14*}, if formed in the intermediate step in the high energy reaction, does not have the same excitation distribution as those formed in low energy proton bombardments, such as $C^{13} + p \rightarrow N^{14*}$. This is expected, since the high energy incident proton, after causing a knock-on (p,pn) reaction, would leave the residual N^{14*} nucleus "disturbed" or "excited" very locally, which is different from the "sharing" or "distributed" excitation in the compound nucleus picture.

d. It should be noted that the energy required to de-bind a neutron from N^{14} is 10.6 Mev, while the amount required to remove a proton is only 7.57 Mev. The low yield of N^{13} nuclide in this work is then compared with the low cross sectional values from other high energy proton interactions, such as from Al^{27} (3). After the initial cascade, e.g., in Al^{27}, further evaporation will, in general, tend toward the stability line. The immediate precurser of N^{13} from high energy reaction probably is N^{14*} with 8 to 16 Mev excitation energy. The 3 Mev binding energy difference, will then favor the formation of C^{13} rather than N^{13}. Thus, this difference in binding energy alone might be sufficient to explain the low yield of N^{13}.

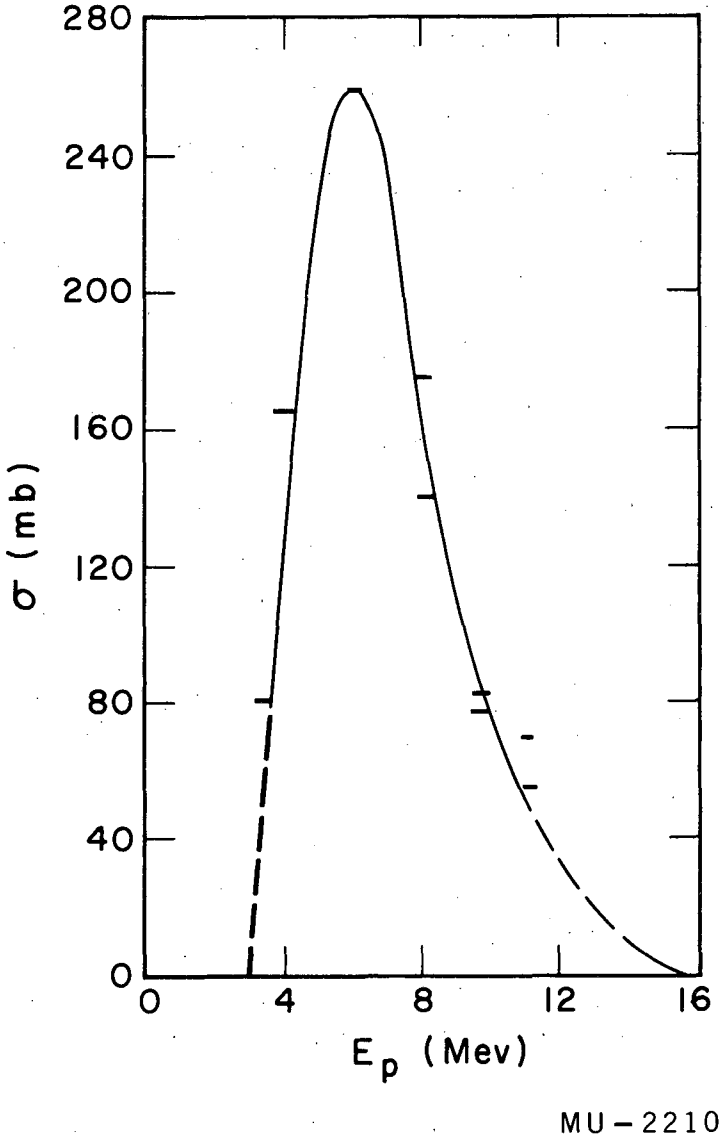

Fig. 10. Excitation of $C^{13}(p,n)N^{13}$ below 12 Mev.

e. The observed slight maximum in both (p,pn) and (p,p2n) reactions (see Table 3 and 4) is not understood at this time. This may possibly be related to the variation in the production cross sections for mesons, their energy distribution and their escape probabilities, as the incident proton energy is increased from 0.4 to 6.2 Bev.

f. To correlate the (p,pn) and the (p,p2n) reaction cross sections more specifically, more experimental data on (p,p2n) reactions are required, especially in the cases where (p,pn) cross sections have already been measured. Some of these are: $Fe^{54}(p,p2n)Fe^{52}$ and $Cu^{63}(p,p2n)Cu^{61}$.

ACKNOWLEDGMENTS

I would like to express my gratitude to Professor S. S. Markowitz under whose guidance this work was performed. I would also like to thank Dr. L. Winsberg for his interest and advice; Health Chemistry for the various assistances; Bevatron and 184-inch synchrocyclotron operating group for their cooperation; L. Schifferle for his help; and Dr. E. Huffman, E. Jeung, D. Sisson for the chemical analysis.

This work was done under the auspices of U. S. Atomic Energy Commission.

REFERENCES

(1) S. S. Markowitz, F. S. Rowland and G. Friedlander, Phys. Rev. 112, 1295 (1958).

(2) J. B. Cummings, G. Friedlander and C. E. Swartz, Phys. Rev. 111, 1386 (1958).

(3) G. Friedlander, J. Hudis and R. L. Wolfgang, Phys. Rev. 99, 263 (1955).

(4) J. L. Symonds, J. Warren and J. D. Young, Proc. Phys. Soc., A, LXX, 824 (1957).

(5) P. Benioff, UCRL-8780, (1959).

(6) D. Barr, unpublished, UCRL, (1956).

(7) N. Metropolis, R. Bivins, M. Storm, J. M. Miller, G. Friedlander and A. Turkevich, Phys. Rev. 110, 204 (1958).

(8) W. Hess and B. Moyer, Phys. Rev. 101, 337 (1956).

(9) I. M. Ladenbauer and L. Winsberg, UCRL-8907 (1959).

(10) N. Horwitz and J. Murray, UCRL-8881 (1959).

(11) L. Marquez, Phys. Rev. 86, 405 (1952).

(12) H. P. Yule and A. Turkevich, Phys. Rev. 118, 1591 (1960).